Zinc Coordination of Carboxylate Surfactomesogens to Poly(4-vinylpyridine)

Mohamed Benouazzane,[†] Elda Bravo-Grimaldo,[‡,§] Rabin Bissessur[⊥,‡,] and C. Geraldine Bazuin*[,†,‡]

Département de chimie, Université de Montréal, C.P. 6128 Succ. Centre-Ville, Montréal (QC), Canada H3C 3J7, and Département de chimie, Université Laval, Cité universitaire, Québec (QC), Canada G1K 7P4

Received February 27, 2006; Revised Manuscript Received May 29, 2006

ABSTRACT: Zinc salts of carboxylic acid-functionalized alkoxybiphenyl mesogens (also termed surfactomesogens), $HO_2C(CH_2)_{n-1}PhPhOCH_3$, $n = 6$ and 11, Ph = phenyl, were melt-blended with poly(4-vinylpyridine), mainly at a mesogen/(vinylpyridine) molar ratio of 0.5, and studied by infrared spectroscopy, differential scanning calorimetry, polarizing optical microscopy, and X-ray diffraction. Melt-blending results in complexation between the two components via zinc coordination (at the same maximal level for $n = 6$ and 11), and the complexes obtained are temporally stable at ambient temperature. The complex with $n = 6$ appears to be simply amorphous, with some excess surfactomesogen in crystalline form. In contrast, the complex with $n = 11$ is mesomorphic, structurally organized as a single-layer smectic A phase at ambient temperature, with no crystallization of excess surfactomesogen. It is concluded that a spacer length of 6 is not sufficient to decouple the biphenyl core from the coordination site so as to permit liquid crystal ordering, whereas this is possible for a spacer length of 11. At temperatures above 100 °C, decomplexation accompanied by crystallization of most of the surfactomesogen occurs in both systems (with complexation obtained again above the melting point). These complexes are the first examples in the literature, to our knowledge, of metal-coordinated comblike polymers involving surfactomesogens (as opposed to simple surfactants) and show the interest of this metallosupramolecular approach for the conception of novel side-chain liquid crystal polymers.

Introduction

Numerous supramolecular side-chain liquid crystal polymers or, more generally, supramolecular comb polymers, where mesogenic or alkyl side chains are "grafted" to linear polymers via noncovalent interactions, have been investigated over the past 15 years or so.[1−8] The great majority of these polymers are based on hydrogen-bonding interactions, followed in number by ionic interactions. Very few of these systems use metal coordination to bind the side chain to the polymer backbone, although it may be expected that this approach could provide more robust materials (depending on the choice of metal and ligands) as well as allow the incorporation of metal-related properties such as luminescence and magnetism. On the other hand, this approach—also called the metallosupramolecular approach—has been employed somewhat more extensively to build main-chain polymers (not necessarily liquid crystalline).[9]

To our knowledge, the only comblike metallosupramolecular polymer systems that have been studied to date bind simple alkyl side chains to polymer backbones through metal−ligand coordination. Belfiore et al. blended zinc laurate with poly(4-vinylpyridine) (P4VP) and obtained homogeneous complexes up to about 30 mol % Zn laurate content, beyond which phase separation sets in.[10] No liquid crystalline properties were reported. Ruokolainen et al. found lamellar liquid crystal organization in complexes of zinc dodecylbenzenesulfonate with either P4VP[11] or polyaniline,[12] including up to equimolar proportions for P4VP. Kurth et al. combined metallosupramolecular main-chain and surfactant side-chain (dihexadecyl phosphate) complexation using iron-based coordination and obtained a material with thermotropic polymorphism.[13] A three-component "multicomb" system was achieved by Valkama et al., in which a trifunctional molecule serves as an intermediary supramolecular element by being simultaneously Zn-coordinated to P4VP and ionically bonded (after proton transfer) to dodecyl benzenesulfonate; this system was observed to self-organize into a hexagonal structure.[14]

In this work, we investigate the possibility of complexing mesogenic molecules to a polymer chain by metal coordination. With mesogenic molecules, much greater versatility in the structure, properties, and functions of the resulting material is possible. The above-mentioned studies based on zinc coordination are used as a starting point. To this end, we chose model mesogens of a type previously (and easily) synthesized by us,[15] namely, carboxylic acid-functionalized alkoxymethoxybiphenyl mesogens ($HO_2C(CH_2)_{n-1}PhPhOCH_3$, where $n = 6$ or 11 and Ph = phenyl) that were converted to zinc salts, and P4VP as the polymer. The mesogens, which we also term surfactomesogens due to their surfactant-like molecular structure,[16] have two different alkyl spacer lengths, since it is well-known that this parameter can strongly influence potential liquid crystal properties.[17] The investigations are confined almost exclusively to the composition where the surfactomesogen is in a 0.5 molar ratio relative to the vinylpyridine repeat unit, given that the study of ref 10 indicates that it is unlikely to obtain full complexation of a Zn carboxylate surfactant to the polymer at higher molar ratios. Yet, if full or nearly full complexation is achieved, this ratio is typically more than enough to obtain liquid crystal character according to studies with all-covalent side-chain liquid crystal copolymers.[18,19]

* To whom correspondence should be addressed. Current address: Université de Montréal. E-mail: geraldine.bazuin@umontreal.ca.
[†] Université de Montréal.
[‡] Université Laval.
[§] Current address: Institute for Biodiagnostics, National Research Council Canada, 435 Ellice Ave., Winnipeg (MB), Canada R3B 1Y6.
[⊥] Current address: Department of Chemistry, University of Prince Edward Island, 550 University Ave., Charlottetown (PE), Canada C1A 4P3.

10.1021/ma060430v CCC: $33.50
Published on Web 07/08/2006

Table 1. Elemental Analyses and DSC-Obtained Melting Points of the Compounds Synthesized

sample	empirical formula		% C	% H	% N	melting point (°C)
LC-1,6A	$C_{19}H_{22}O_4$	calcd	72.61	7.01		
		found	72.64	7.28		160
LC-1,11A	$C_{24}H_{32}O_4$	calcd	75.00	8.33		
		found	75.53	8.20		162
LC-1,6Z	$C_{38}H_{42}O_8Zn$	calcd	65.95	6.07		
		found	65.72	5.86		264
LC-1,11Z	$C_{48}H_{62}O_8Zn$	calcd	69.28	7.55		
		found	69.09	7.75		228
LC-1,6Z/P4VP	$C_{66}H_{70}O_8N_4Zn{\cdot}H_2O$	calcd	70.13	6.38	4.96	
(0.5 molar ratio)	after melt	found	70.20	6.49	4.83	227
LC-1,11Z/P4VP	$C_{76}H_{90}O_8N_4Zn{\cdot}H_2O$	calcd	71.84	7.25	4.41	
(0.5 molar ratio)	before melt	found	71.30	7.83	4.01	
	after melt	found	71.54	7.26	4.00	212

Scheme 1. P4VP + LC-1,*n*Z, *n* = 6, 11

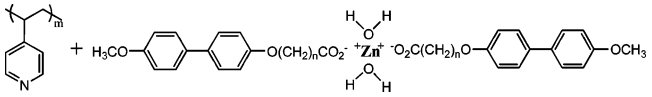

Experimental Section

Synthesis and Characterization of LC-1,*n*Z, *n* = 6, 11. The carboxylic acid surfactomesogens (labeled LC-1,*n*A, where $n = 6$ and 11 designates the number of carbons in the alkyl spacer plus that of the acid group, "1" designates the single carbon in the methoxy tail, and A designates the acid form) were synthesized as described previously for a similar compound.[15] They were converted to Zn salts (labeled LC-1,*n*Z) in anhydrous ethanol under reflux conditions using zinc acetate dihydrate, $Zn(CH_3COO)_2{\cdot}2H_2O$. Full neutralization was verified by infrared spectroscopy, which showed the complete disappearance of the carbonyl band near 1700−1710 cm^{-1} as well as of the broad acid band at 3200 cm^{-1} and the appearance of the asymmetric and symmetric carboxylate bands near 1550 cm^{-1} (1555 cm^{-1} for $n = 6$ and 1542 cm^{-1} for $n = 11$) and in the 1400−1450 cm^{-1} range, respectively.[20] Elemental analyses and melting points of the compounds are given in Table 1. It is notable that the melting points of the Zn-neutralized mesogens depend on the alkyl chain length, whereas no such dependence is observed for the acid-functionalized mesogens.

LC-1,6A. ^{1}H NMR (Bruker, 400 MHz, Pyr-d_5): $\delta = 7.63$ (4H, 2d, Ar), 7.10 (2H, d, Ar), 7.07 (2H, d, Ar), 3.93 (2H, t, OCH_2), 3.69 (3H, s, OCH_3), 2.51 (2H, t, CH_2-acid), 1.79 (4H, m, CH_2), 1.56 (2H, m, CH_2). **LC-1,6Z**. ^{1}H NMR (Bruker, 400 MHz, Pyr-d_5): $\delta = 7.62$ (8H, 2d, Ar), 7.07 (8H, 2d, Ar), 3.90 (4H, t, OCH_2), 3.69 (6H, s, OCH_3), 2.63 (2H, t, CH_2-acid), 1.90 (4H, m, CH_2), 1.76 (4H, m, CH_2), 1.56 (4H, m, CH_2). **LC-1,11A**. ^{1}H NMR (Bruker, 400 MHz, Pyr-d_5): $\delta = 7.66$ (2H, d, Ar), $\delta = 7.64$ (2H, d, Ar), 7.15 (2H, d, Ar), 7.08 (2H, d, Ar), 3.97 (2H, t, OCH_2), 3.70 (3H, s, OCH_3), 2.51 (2H, t, CH_2CO_2), 1.76 (4H, m, CH_2), 1.31 (4H, m, CH_2), 1.22 (8H, m, CH_2). **LC-1,11Z**. ^{1}H NMR (Bruker, 400 MHz, Pyr-d_5): $\delta = 7.65$ (4H, d, Ar), $\delta = 7.64$ (4H, d, Ar), 7.15 (4H, d, Ar), $\delta = 7.07$ (4H, d, Ar), 3.97 (4H, t, OCH_2), 3.70 (6H, s, OCH_3), 2.64 (4H, t, CH_2CO_2), 1.89 (4H, m, CH_2), 1.73 (4H, m, CH_2), 1.40 (8H, m, CH_2), 1.20 (16H, m, CH_2).

Preparation of LC-1,*n*Z/P4VP Mixtures. Since a common solvent that completely dissolved both components and led to successful complexation could not be found,[21] they were mixed in two steps: first, a finely dispersed mixture was obtained from solution, and subsequently this mixture was melt-blended. Specifically, appropriately calculated amounts of the two components, LC-1,*n*Z and P4VP (Fisher Scientific, $M_w = 200\,000$, used as received), were initially dispersed and dissolved, respectively, in anhydrous ethanol, chosen for its nontoxicity and easy evaporation. The clear P4VP solution was added dropwise to the cloudy LC-1,*n*Z solution under reflux, giving a milky solution that was refluxed overnight, and then concentrated by rotary evaporation. The product was finely precipitated by dropwise addition of hexane to the concentrated solution, followed by filtration and drying in a 60 °C vacuum oven for 2 days. It was also efficient to simply allow the ethanol to evaporate at ambient temperature for a day, followed by drying in the vacuum oven.

Subsequently, the mixtures were hot-blended in specially made small glass vials on a Köffler heating bench (Wagner & Munz) just above the melting point of the mesogen. As the melting proceeded, the initially white powder turned reddish.[22] After kneading the (pasty) melt for the desired time, the vial was simply removed from the heating element. All prepared mixtures were placed for at least 24 h in a 60 °C vacuum oven and then, if not used immediately for measurements, were stored in a desiccator containing $CaCl_2$.

The NMR spectra of the complexes are simply a superposition of the two components (with broad peaks for the polymer), and they are identical both before and after melt-blending. Elemental analyses of the complexes, given in Table 1, are very satisfactory when one H_2O molecule per Zn (or 0.25 H_2O per VP moiety, which corresponds to 0.5 H_2O per uncomplexed VP if maximum complexation is achieved) is included in the calculated values; it is notable that the results for the mixtures before and after melt-blending (tested for $n = 11$) are very close. Thermogravimetric analysis of the $n = 11$ sample indicates that weight loss for the unmelted mixture only begins at about 270 °C (1% weight loss), consistent with the visual observation that when the sample is exposed to temperatures significantly above the melting point, the reddish color turns to brown. Finally, a melt-blended complex was dissolved in pyridine and redried, after which it again became creamy white in color,[22] and its infrared spectrum was close to that for the mixture before melt-blending (see Results), showing the reversibility of the complexation reaction. All of these data support the absence of undesired chemical reaction or degradation during melt-blending just above the melting point.

Instrumentation. Infrared spectra of samples ground with dry KBr and pressed into pellets were recorded at ambient temperature with a Digilab FTS 3100 HE mid-IR Excalibur or a Nicolet Magna IR 560 spectrometer. Thermogravimetric analysis (TGA) was carried out using a TA Instruments Hi-Res TG2950 or a Mettler TG50 instrument; the samples were scanned at a rate of 10 °C/min under N_2 flow.

Differential scanning calorimetry (DSC) was performed using a Perkin-Elmer DSC-7 calorimeter, calibrated with indium and flushed with N_2. About 10 mg of sample was packed in standard aluminum pans (in graphite pans for the data shown in Figure S2 in the Supporting Information). The samples were scanned at a rate of 10 °C/min. First-order transition temperatures are given by the peak values and glass transition temperatures by the midpoint of the heat capacity jump. Polarizing optical microscopy (POM) observations of the samples were made with a Zeiss Axioskop microscope equipped with a 25X Leica objective. The temperature was regulated using a Mettler FP5 temperature controller and FP52 hot stage.

X-ray diffraction (XRD) analysis was carried out with a Bruker D8 Discover diffractometer system with GADDS, equipped with a Kristalloflex K760-80 generator and a Hi-Star detector system, using filtered Cu Kα radiation. Powder samples were sealed in Lindemann capillaries (Charles Supper) of 1.0 mm i.d. Temperature was regulated by an Instec HCS410 hot stage and a STC200

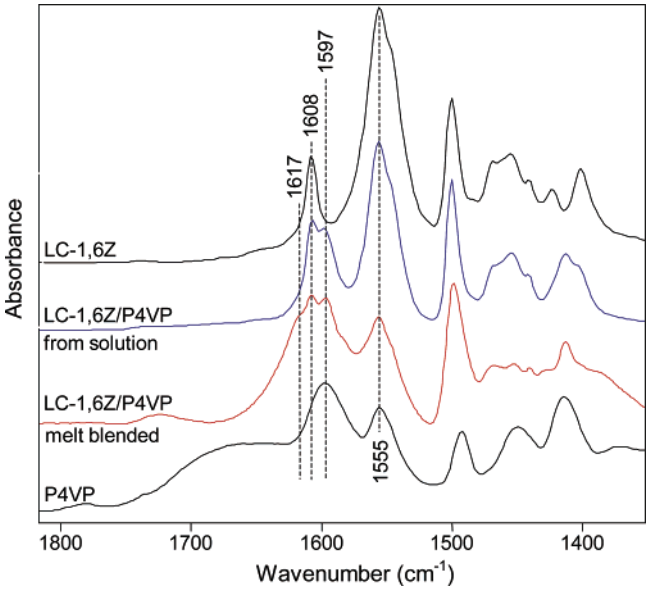

Figure 1. FTIR spectra of the equimolar LC-1,6Z/P4VP complex before and after melt-blending, compared with pure LC-1,6Z and pure P4VP.

controller. Only heating was controlled; cooling took place at a natural rate, which decreased with decreasing temperature. All profiles were treated by subtracting a baseline profile obtained with an empty capillary tube. The *d*-spacing was determined from the maximum of low-angle diffractions peaks in the smoothed diffractograms, using Bragg's relation, $d = n\lambda/(2 \sin \theta)$, where n is the diffraction order, 2θ the diffraction angle, and λ the wavelength equal to 1.542 Å. The calculated molecular length, l, was estimated using Hyperchem 5.0 (Hypercube Inc.), assuming most extended conformations and including van der Waals' radii at the extremities.

Results and Discussion

Conditions and Evidence for Complexation. Evidence to determine whether there is complexation between LC-1,*n*Z and P4VP can be obtained from FTIR. The absorption band at 1597 cm^{-1} for P4VP, a pyridine ring stretching mode, is well-known to shift to higher wavenumbers when the VP moiety is hydrogen-bonded, ionized, or metal-coordinated. In the present case, a vibration band at 1608 cm^{-1} characteristic of the biphenyl moiety in the mesogen complicates matters. Fortunately, Zn coordination to P4VP shifts the pyridine absorption band to 1617 cm^{-1},[10,11] which is sufficiently removed from the biphenyl absorption that it should be clearly visible.

In Figure 1, the spectrum corresponding to the LC-1,6Z/P4VP mixture obtained from solution (before melt-blending) shows no evidence of a band near 1617 cm^{-1}, but instead appears to be essentially a superposition of the two spectra corresponding to the pure components. However, following up on preliminary DSC data indicating a steadily decreasing melting point with each subsequent scan (restricted to a maximum temperature a little beyond the melting point) and the observation that the contents of the DSC pan had turned reddish, it was discovered that the IR spectrum does show absorption in the 1617 cm^{-1} region after melting, which led to the adoption of the melt-blended preparation procedure. This absorption is clearly observed in the spectrum of the melt-blended sample in Figure 1, in the form of a shoulder on the higher wavenumber side of the composite band around 1600 cm^{-1}. Simultaneously, the asymmetric carboxylate absorption[20] with a maximum at 1555 cm^{-1} decreases strongly in intensity, with its remaining presence weakly indicated by the 1542 cm^{-1} shoulder[20] on the low wavenumber side of the pyridine band at 1556 cm^{-1}. Changes

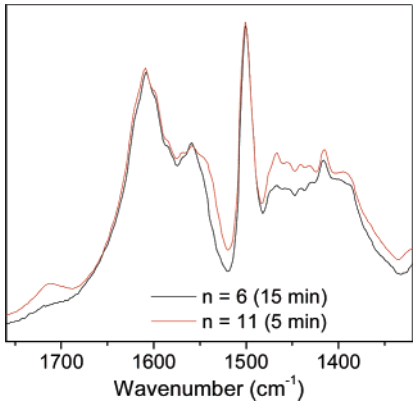

Figure 2. Infrared spectra comparing the maximally complexed LC-1,*n*Z/P4VP mixtures (achieved at the melt-blending times indicated; see text for details).

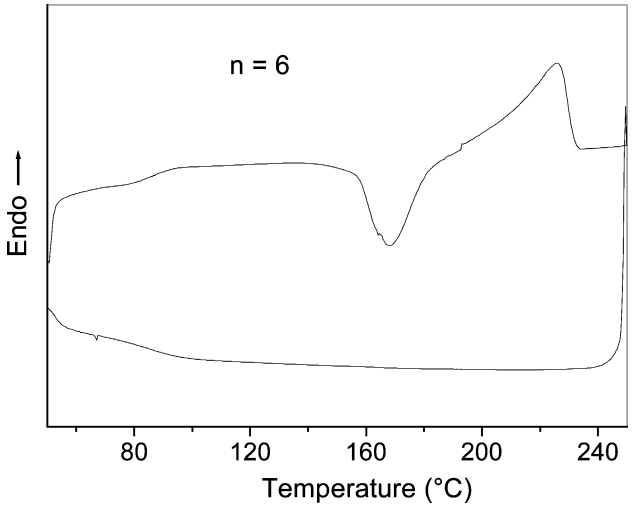

Figure 3. DSC thermograms (first heating and cooling scans) of the 0.5 LC-1,6Z/P4VP 15 min melt-blended mixture.

in the region of the symmetric carboxylate band, as well as in other regions of the spectra, are also apparent. All of these changes are consistent with a modification of the Zn carboxylate coordination structure to one involving pyridine. A low-intensity band near 1710 cm^{-1} suggests that a small amount of acid groups has been regenerated, which may give rise to acid-salt structures that can contribute as well to changes in the carboxylate bands;[23] monodentate carboxylate formation is another possibility.

Once it was established that some degree of complexation is achieved by melt-blending, it was necessary to determine the length of time necessary for maximum complexation. To this end, samples were subjected to the melt-blending procedure for variable amounts of time, and their infrared spectra were taken. These spectra are given in the Supporting Information, where it is shown that about 15 min in the melt is necessary for $n = 6$ and at most 5 min for $n = 11$. Figure 2 compares the spectra of the two systems after those melt-mixing times: they indicate that the level of maximal complexation achieved appears similar in both systems.

LC-1,6Z/P4VP Complexation. DSC thermograms (first heating and cooling curves) for the 0.5 molar ratio LC-1,6Z/P4VP melt-blended sample are given in Figure 3. The heating thermogram shows a glass transition at 85 °C (indicative of plasticization of P4VP by complexed mesogen), recrystallization near 170 °C, and a melting point at 227 °C, the last being about 40 °C lower than that of the surfactomesogen alone. Subsequent

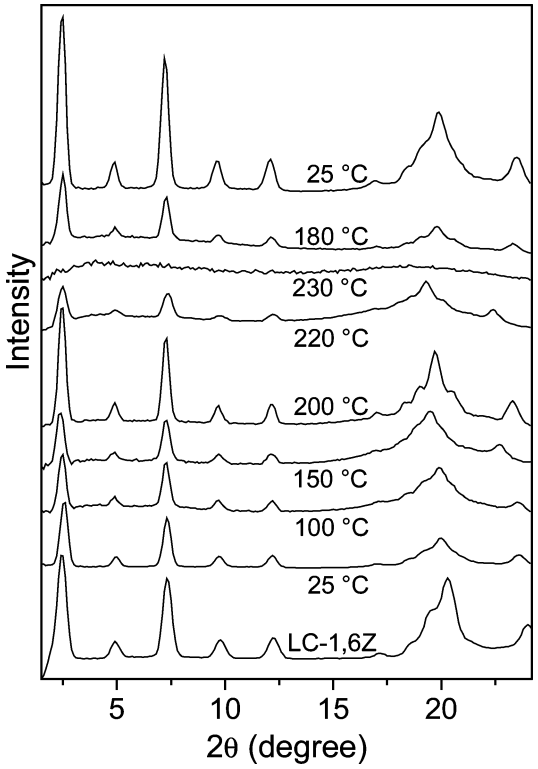

Figure 4. X-ray diffractograms of pure LC-1,6Z at ambient temperature and of the 15 min melt-blended 0.5 LC-1,6Z/P4VP complex at the temperatures indicated, taken in order from bottom to top. The changes in relative intensities for the complex qualitatively reflect real changes (see text).

heating curves (both after cooling at 10 °C/min and after quenching) are very similar, except that the T_g increases by about 15 °C and recrystallization occurs in a temperature range about 10 °C higher. There are no exothermic events in the cooling curves. Polarizing optical microscopy indicates that the complex is isotropic after melting, and crystallization on cooling occurs very slowly. DSC thermograms of melt-blended LC-1,6Z/P4VP mixtures of various molar ratios, given and commented on in the Supporting Information, illustrate in more detail the glass transition and crystallization behavior in these complexes. This behavior is consistent with the presence of some degree of complexation and suggests that the crystallization is related to uncomplexed mesogen.

X-ray diffractograms at various temperatures for the 0.5 sample are shown in Figure 4. Examining first the diffractogram of the as-prepared sample at ambient temperature, it is observed that the number of low-angle reflection orders (five), the pattern of their relative intensities (more intense for the odd-numbered reflections), their *d* spacings, and the wide-angle pattern are essentially the same as for pure LC-1,6Z, also shown. The wide-angle pattern is indicative of an ordered (i.e., crystalline) structure, and the equidistant spacing of the low-angle reflections shows that this structure is lamellar in nature. The *d* spacing (36 Å) of the first-order peak corresponds to the estimated length of two extended surfactomesogens coordinated in a linear fashion to a single Zn ion.[24] It can thus be supposed that the Zn-coordinated mesogens are aligned perpendicularly to the lamellar planes of the crystalline structure. This structure remains essentially unmodified at higher temperatures (until melting, shown by the 230 °C diffractogram), except for some in-plane rearrangement and changes in overall intensities, and it reappears on cooling from the melt. The effect of recrystallization on heating is clearly visible by the increased intensity and the wide-angle modifications in the diffractogram taken at 200 °C on heating compared to the one taken at 150 °C.

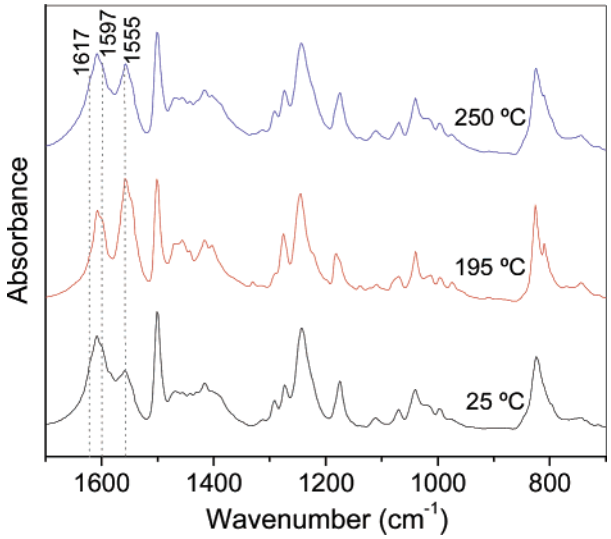

Figure 5. Infrared spectra at ambient temperature of the 0.5 LC-1,-6Z/P4VP complex after the melt-blending preparation (labeled as 25 °C) and after heating to 195 and 250 °C. The rate of heating and cooling for the last two samples was 10 °C/min.

The data strongly suggest that the ordered phase should be attributed to excess uncomplexed LC-1,6Z. If it were to arise from the LC-1,6Z/P4VP complex, the *d* spacing would be expected to change compared to pure LC-1,6Z, and a significant modification other than a simple increase in intensity would be expected above the temperature region of recrystallization on heating (or otherwise, the polymer chain must somehow be intercalated within the crystalline arrangement of the surfactomesogens without modifying either the lamellar thickness or the in-plane order, which seems unlikely). That no crystallization is observed in the DSC cooling curves, but is during XRD cooling[25] and after the melt-blending procedure, can be related to the slow crystallization rate of the uncomplexed mesogen in the presence of the complex (with which it is probably miscible in the melt state, as deduced from the DSC data; see the Supporting Information).

To probe the state of complexation after different thermal histories, infrared spectra were taken of the sample after it was heated to selected temperatures and then cooled under the DSC conditions (10 °C/min). These spectra are shown in Figure 5. Compared to the spectrum of the melt-prepared sample (identified as 25 °C), that of the sample that was heated to a temperature between the recrystallization and melting ranges (195 °C) clearly shows that recrystallization is followed by considerable reduction in complexation. (Comparison with the spectrum of the solution-prepared sample suggests, however, that residual complexation remains.) After heating the complex to the melt region and slow cooling (10 °C/min), the spectrum again resembles that obtained from the melt-prepared sample, confirming that complexation occurs in the melt and showing that it is maintained even during fairly slow cooling. (However, the greater intensity of the peak at 1556 cm^{-1} in this spectrum compared to the original one indicates that the extent of complexation is somewhat less than in the melt-prepared sample, which had undergone faster cooling.) It also illustrates that the degree of complexation can be controlled by thermal manipulation.

The following picture can now be drawn for this system. Complexation of the surfactomesogen to P4VP by zinc coordination proceeds in the melt and can be frozen in quite easily.

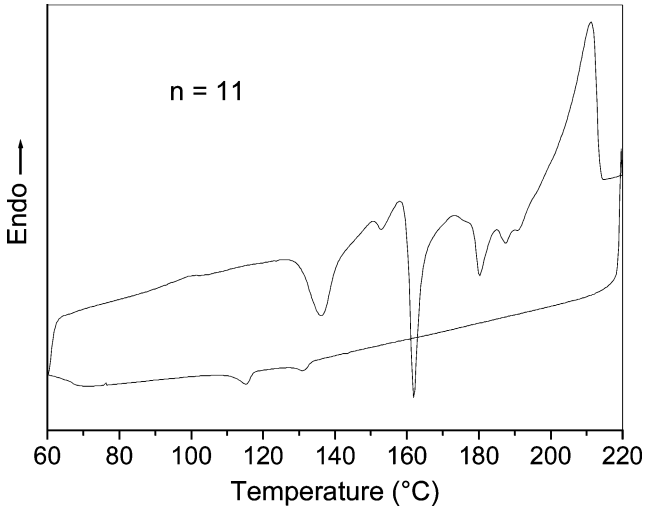

Figure 6. DSC thermograms (first heating and cooling scans) of the 0.5 LC-1,11Z/P4VP 5 min melt-blended mixture.

This complex, although thermodynamically metastable, is temporally stable at ambient temperature, with decomplexation, accompanied by (or driven by) recrystallization, occurring at much higher temperature than ambient. There is no evidence of any liquid crystal phase for this system. Considering that the crystalline structure observed by XRD is associated with excess uncomplexed LC-1,6Z, then it must be concluded that the complex itself is simply amorphous. This amorphous character may be the result of a degree of complexation that is insufficient to give rise to a liquid crystal side-chain copolymer, as has been observed previously in analogous hydrogen-bonded supramolecular complexes.[15] Alternatively, the alkyl spacer that permits decoupling of the mesogenic core from the Zn-coordinated polymer backbone is too short to allow liquid crystal ordering. The next section will indicate that this latter explanation is the most likely one.

LC-1,11Z/P4VP Complexation. The DSC thermograms of the LC-1,11Z/P4VP melt-blended mixture, given in Figure 6, show a complex series of exotherms and endotherms during heating, with a final melting peak at 212 °C (which is again significantly lower than the melting point of pure LC-1,11Z). On cooling, only two weak transitions are observed at 134 and 118 °C, respectively. These thermograms are essentially reproducible on repeated scans, whether cooled at 10 °C/min or quenched. No glass transition is clearly visible, although the cooling curve suggests that it is near 65 °C. (It is expected that it should be lower than for the $n = 6$ complex at a similar degree of complexation, due to greater internal plasticization by the longer effective side chains, at least if the same amorphous structure is obtained.)

Interestingly, POM observations indicate that melting is accompanied by a birefringent liquid phase (easily shearable) that is reminiscent of a disordered liquid crystal mesophase. This phase was observed to be stable over about a 10 °C interval before the isotropic phase appeared at about 213 °C. It is also very stable over time when heating is arrested in this phase. Upon cooling from the isotropic phase, this liquid birefringent phase reappeared only after a long time at a fixed temperature a few degrees below isotropization (e.g., 1−2 h at 205 °C). However, no tell-tale texture permitting identification of this mesophase could be obtained (a photomicrograph is given in the Supporting Information). Crystallization was also observed to be very slow. When cooling from the isotropic phase at 10 °C/min, the sample showed no birefringence until the 140−130 °C region was reached (this is also where weak DSC peaks occur on cooling), when numerous small birefringent dots appeared, indicative of a small amount of crystallization or reappearance of a liquid crystalline phase. No further change was noted on continued cooling to ambient temperature.

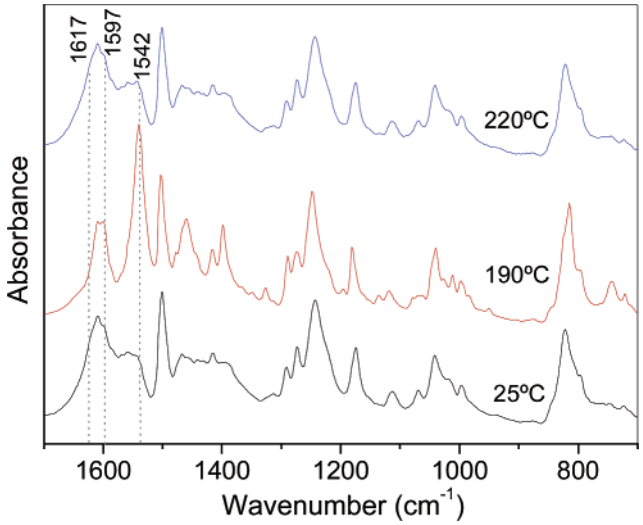

Figure 7. Infrared spectra at ambient temperature of the 0.5 LC-1,-11Z/P4VP complex after the melt-blending preparation (labeled as 25 °C) and after heating to 190 and 220 °C. The rate of heating and cooling for the last two samples was 10 °C/min.

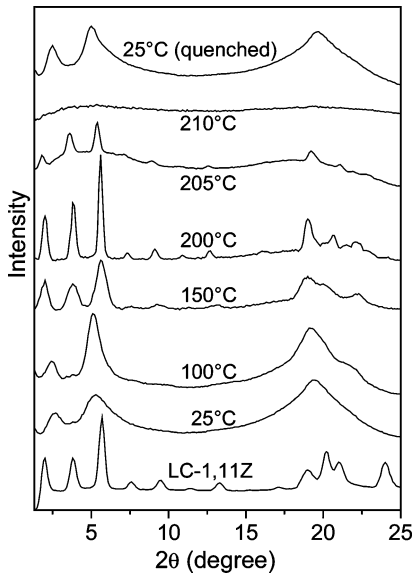

Figure 8. X-ray diffractograms of pure LC-1,11Z at ambient temperature and of the 5 min melt-blended 0.5 LC-1,11Z/P4VP complex at the temperatures indicated, taken in order from bottom to top. The relative intensities of the curves have been adjusted for ease of viewing.

From the infrared spectra of samples heated to selected temperatures and cooled (Figure 7), it is again observed that the recrystallization on heating is accompanied by extensive decomplexation (190 °C spectrum, which is quite similar to the spectrum of the solution-obtained sample) and that recomplexation takes place in the melt and is maintained even after fairly slow cooling (220 °C spectrum, which is almost identical to the 25 °C spectrum).

X-ray diffractograms at various temperatures are given in Figure 8. This time, the ambient-temperature pattern of the as-prepared melt-blended sample is very different from that of the corresponding mesogen (also given in Figure 8). It is characterized by two relatively broad peaks in the lower angle region[26]—

corresponding to *d* spacings of 34 and 17 Å, respectively, and thus indicative of lamellar order—and a broad halo near 20° (4.5 Å). Since this spacing is similar to the estimated molecular length of a single, fully extended LC-1,11Z molecule complexed to a 4VP unit, it may be deduced that the structure is essentially that of the complex in the form of a single-layer (or fully interdigitated) smectic A mesophase.

This structure appears to improve its order on heating to 100 °C (sharper and more intense low angle peaks), with possible low in-plane or crystalline order also developing as shown by the weak diffraction appearing near 23° (which may be related to the weak endotherm observed in the DSC heating thermogram near 100 °C or the beginning of crystallization). By 150 °C, the liquid crystal order is lost, and lamellar crystalline order very similar to that of the pure surfactomesogen is apparent. The latter structure clearly improves at higher temperatures, as indicated by the more intense and sharp peaks at 200 °C. This is consistent with the infrared data showing decomplexation and the DSC data showing recrystallization between about 130 and 200 °C. That melting occurs between about 200 and 210 °C is clearly reflected in the diffractograms obtained at 205 and 210 °C. The fact that no evidence for another structure could be observed by XRD between 205 and 210 °C might indicate that the liquid crystalline phase clearly seen by POM in this region is a nematic mesophase, which gives a diffractogram similar to that of an amorphous phase.

When the sample is cooled quickly to ambient temperature, the diffractogram [labeled 25 °C (quenched) in Figure 8] is again like that of the initial diffractogram and consistent with recomplexation having occurred in the melt. On the other hand, if the sample is cooled slowly from the melt (at 10 °C/min, with pauses at 180 and 150 °C for the recording of diffractograms, which amounts to annealing in temperature regions where crystallization can occur according to the DSC results, as noted in ref 25 for $n = 6$), diffractograms indicating that crystallization has taken place, including at 180 °C, are obtained (not shown). The *d* spacings for the crystallized sample are close to that for the pure surfactomesogen (48 Å), consistent with the crystallization being associated with decomplexed LC-1,11Z, and indicate an orthogonal bilayer lamellar crystalline phase, as for LC-1,6Z.

The picture that emerges for the LC-1,11Z/P4VP mixture is, in part, similar to that for the $n = 6$ mixture, in that a temporally stable but thermodynamically metastable complexed copolymer is obtained from the melt, with decomplexation taking place at temperatures much higher than ambient. However, this time the complexed copolymer is not amorphous but liquid crystalline. Furthermore, there is no evidence of crystallized uncomplexed mesogen, contrary to the $n = 6$ mixture, although the infrared spectra of the maximally complexed LC-1,nZ/P4VP mixtures indicate a similar level of complexation for $n = 6$ and 11 (Figure 2). This implies that some uncomplexed mesogen must also remain in the maximally complexed $n = 11$ system. If so, it must be concluded that its crystallization is slowed down even more than in the $n = 6$ system (qualitatively supported by POM observations), which may be related to its longer alkyl chain (disordered in the melt) or to the liquid crystalline nature of the $n = 11$ complex (with which the uncomplexed mesogen may be miscible, as deduced for $n = 6$ in the melt state).

It must also then be concluded that it is the spacer length and not the degree of complexation that makes the difference in the nature of the two complexes, such that for $n = 11$ it is liquid crystalline and for $n = 6$ it is amorphous. In other words, decoupling of the mesogenic units from the zinc-complexed backbone by 6 CH_2's is not sufficient to permit the development of liquid crystal order. It may be noted, in this connection, that a minimum spacer length of 8 CH_2's was observed to be necessary in pyridinium tail-end polymethacrylates for (smectic A-like) lamellar ordering to begin to be observed.[27]

Conclusions

Carboxylic acid surfactomesogens can be successfully coordinated by zinc to poly(4-vinylpyridine) through a melt-blending process. The maximum extent of coordination possible appears to somewhat less than 0.5 acid/pyridine molar ratio, giving supramolecular Zn-coordinated side-chain copolymers. The extent of complexation is nevertheless enough to result in liquid crystalline systems when the spacer length is sufficient to decouple the rigid mesogenic core from the coordination site. In the present case, for maximal complexation, it appears that a spacer length of 6 methylene units is too short, giving an amorphous complex, whereas a spacer length of 11 leads to a single-layer, smectic A-like mesophase (and possibly a nematic mesophase at high temperatures). The complexes obtained are temporally stable at ambient temperature. On the other hand, they are thermodynamically metastable, but decomplexation and crystallization of the surfactomesogen occur only at elevated temperatures (well above 100 °C). Thus, this is a promising approach for a new class of liquid crystalline materials, in which interesting mesogenic characteristics, such as chirality or optical responsiveness, can be combined with metal-related properties. Possibly, if the tendency for the (Zn-carboxylated) surfactomesogens to crystallize is reduced, thermodynamically stable complexes can be obtained. On the basis of refs 11 and 12, it may also be expected that Zn-sulfonated surfactomesogens may lead to much greater and possibly thermodynamically stable complexation.

Acknowledgment. The financial support of NSERC (Canada), FCAR/FQRNT (Québec), and Université de Montréal is gratefully acknowledged. R.B. was partially supported by the postdoctoral program of the Centre de recherche en sciences et ingénierie des macromolécules (CERSIM, Université Laval). E.B.G., R.B., and C.G.B. acknowledge their former membership in the CERSIM. M.B. and C.G.B. acknowledge their membership in the multiuniversity Centre for Self-Assembled Chemical Structures (CSACS).

Supporting Information Available: Infrared spectra for the determination of melt-blending times necessary for maximum complexation; DSC data for LC-1,6Z/P4VP mixtures of various molar ratios; POM photomicrograph of the LC-1,11Z/P4VP mixture in its liquid crystalline state. This material is available free of charge via the Internet at http://pubs.acs.org.

References and Notes

(1) Kato, T. *Struct. Bonding (Berlin)* **2000**, *96*, 95 and references therein. Kato, T. In *Handbook of Liquid Crystals*; Demus, D., Goodby, J. W., Gray, G. W., Spiess, H. W., Vill, V., Eds.; Wiley-VCH: Weinheim, 1998; Vol. 2B, p 969; and references therein.

(2) Bazuin, C. G. In *Mechanical and Thermophysical Properties of Polymer Liquid Crystals*; Brostow, W., Ed.; Chapman and Hall: London, 1998; Vol. 3, Chapter 3; and references therein.

(3) (a) Paleos, C. M.; Tsiourvas, D. *Liq. Cryst.* **2001**, *28*, 1127 and references therein. (b) Paleos, C. M.; Tsiourvas, D. *Angew. Chem., Int. Ed. Engl.* **1995**, *34*, 1696 and references therein.

(4) Binnemans, K. *Chem. Rev.* **2005**, *105*, 4148.

(5) Lee, C. M.; Griffin, A. C. *Macromol. Symp.* **1997**, *117*, 281 and references therein.

(6) Antonietti, M.; Thünemann, A. *Curr. Opin. Colloid Interface Sci.* **1996**, *1*, 667 and references therein.

(7) MacKnight, W. J.; Ponomarenko, E. A.; Tirrell, D. A. *Acc. Chem. Res.* **1998**, *31*, 781 and references therein.
(8) Zhou, S.; Chu, B. *Adv. Mater.* **2000**, *12*, 545 and references therein.
(9) See, for example: Caruso, U.; Roviello, A.; Sirigu, A. *Macromolecules* **1991**, *24*, 2606. Marcos, M.; Oriol, L.; Serrano, J. L. *Macromolecules* **1992**, *25*, 5362. Dobrawa, R.; Würthner, F. *J. Polym. Sci., Part A: Polym. Chem.* **2005**, *43*, 4981. Beck, J. B.; Ineman, J. M.; Rowan, S. J. *Macromolecules* **2005**, *38*, 5060.
(10) Belfiore, L. A.; Pires, A. T. N.; Wang, Y.; Graham, H.; Ueda, E. *Macromolecules* **1992**, *25*, 1411.
(11) Ruokolainen, J.; Tanner, J.; ten Brinke, G.; Ikkala, O.; Torkkeli, M.; Serimaa, R. *Macromolecules* **1995**, *28*, 7779.
(12) Ruokolainen, J.; Eerikäinen, H.; Torkkeli, M.; Serimaa, R.; Jussila, M.; Ikkala, O. *Macromolecules* **2000**, *33*, 9272.
(13) Kurth, D. G.; Meister, A.; Thünemann, A. F.; Förster, G. *Langmuir* **2003**, *19*, 4055.
(14) Valkama, S.; Lehtonen, O.; Lappalainen, K.; Kosonen, H.; Castro, P.; Repo, T.; Torkkeli, M.; Serimaa, R.; ten Brinke, G.; Leskelä, M.; Ikkala, O. *Macromol. Rapid Commun.* **2003**, *24*, 556.
(15) Brandys, F. A.; Bazuin, C. G. *Chem. Mater.* **1996**, *8*, 83.
(16) Tibirna, C. M.; Bazuin, C. G. *J. Polym. Sci., Part B: Polym. Phys.* **2005**, *43*, 3421.
(17) McArdle, C. B., Ed.; *Side Chain Liquid Crystal Polymers*; Blackie: Glasgow, 1989.
(18) (a) Percec, V.; Pugh, C. In *Side Chain Liquid Crystal Polymers*; McArdle, C. B., Ed.; Blackie: Glasgow, 1989; p 89. (b) Pugh, C.; Kiste, A. L. In *Handbook of Liquid Crystals*; Demus, D., Goodby, J. W., Gray, G. W., Spiess, H. W., Vill, V., Eds.; Wiley-VCH: Weinheim, 1998; Vol. 3, pp 192−193.
(19) Bazuin, C. G.; Boivin, J.; Tork, A.; Tremblay, H.; Bravo-Grimaldo, E. *Macromolecules* **2002**, *35*, 6893.
(20) The carbonyl band in LC-1,6A is dominated by the acid dimer at 1701 cm^{-1}, whereas in LC-1,11A it is a composite of the acid dimer and a free carbonyl form at about 1710 cm^{-1}. Conversely, the asymmetric carboxylate band in LC-1,11Z is centered at 1542 cm^{-1}, whereas that in LC-1,6Z is dominated by a band at 1555 cm^{-1} accompanied by a shoulder near 1542 cm^{-1}.
(21) DMF and DMSO, for example, dissolved both components but did not lead to complexation. A solvent mixture of dioxane/ethanol (4/1 v/v) also dissolved both components but mainly led to zinc-coordinated P4VP and regenerated acid surfactomesogen.
(22) The change in color to red during melt-blending occurs under both ambient and N_2 atmosphere. It was not observed for either pure LC-1,*n*Z or P4VP or for mixtures of P4VP with Zn acetate or Zn laurate in the same temperature region. It was also observed that dissolution of the melt-blended complexes (but not the unmelted complexes) in pyridine gives a red solution; however, when dried, they are creamy white in color, as before melt-blending, showing its reversibility. We thus presume that the color is related somehow to the particular (local) coordination structure achieved, which may be influenced by the packing requirements of the coordinated surfactomesogen.
(23) Brandys, F. A.; Masson, P.; Guillon, D.; Bazuin, C. G. *Macromol. Chem. Phys.* **2001**, *202*, 856.
(24) Zn−carboxylate distances for the crystal structure of zinc acetate dihydrate are given in: van Niekerk, J. N.; Schoening, F. L. R.; Talbot, J. H. *Acta Crystallogr.* **1953**, *6*, 720.
(25) It should be mentioned that the extent of crystallization observed by XRD after cooling (Figure 4) may well be greater than obtained in the DSC and IR cooling conditions, as suggested also by the X-ray diffractograms at 180 and 25 °C after melting. This can be explained by the fact that the cooling, while ostensibly at 10 °C/min until slower natural cooling set in at lower temperatures, was arrested at the temperatures where measurements were taken. In particular, the measurement at 180 °C amounts to annealing precisely in the zone where crystallization occurs on heating according to DSC (the X-ray beam might also influence crystallization).
(26) It may be noted that the first-order reflection is considerably weaker than the second-order one. This has been regularly observed in the literature and is generally attributed to an additional plane of symmetry in the lamellar electron density profile (see, for example, ref 16 and references therein).
(27) Vuillaume, P. Y.; Bazuin, C. G.; Galin, J.-C. *Macromolecules* **2000**, *33*, 781. Köberle, P.; Laschewsky, A. *Macromolecules* **1994**, *27*, 2165.

MA060430V